

Self-Adaptive Intermediate Resonator in a 3-coil Inductive Link for Power and Data Transmission

Andrés Seré[✉], *Student Member, IEEE*, Leonardo Steinfeld[✉], *Member, IEEE*,
Simon Hemour[✉], *Senior Member, IEEE*, and Pablo Pérez-Nicoli[✉], *Senior Member, IEEE*

Abstract—This paper presents an innovative approach that dynamically adapts the intermediate resonator to enable efficient transmission of power and data over the same inductive link. The proposed intermediate resonator presents a tuned and high-Q response during power transmission, promoting high efficiency in the link. However, when the data transmission begins, it automatically adjusts its response to enable proper communication. Two different approaches for modifying the resonator response during data transmission are tested: 1) dynamically reducing the quality factor, and 2) dynamically detuning the resonator. The proposed resonator is designed, implemented, and applied to an actual commercial system to demonstrate its effectiveness. The selected proof-of-concept system is a low-frequency RFID link, widely used for cattle identification. Detuning the resonator, instead of reducing its quality factor, during data transmission was demonstrated to achieve greater reading distances. Measurements results show that the proposed resonator increases the RFID reading distance by up to $\approx 300\%$ (from 16 cm to 65 cm) compared to not using a resonator, and up to $\approx 50\%$ (from 43 cm to 65 cm) compared to using a regular resonator without the proposed dynamic adaptation. Hence, this study validates the concept of employing batteryless self-adaptive resonators in inductive power links.

Index Terms—wireless power transfer, 3-coil link, RFID, inter-symbol interference (ISI)

I. INTRODUCTION

INDUCTIVE coupling is the most commonly used method for wirelessly transferring energy over short distances. For instance, among its many applications, it is widely used for active implantable medical devices (AIMDs) [1]–[3] and for low and high-frequency radio frequency identification (RFID) [4]. The use of intermediate resonators (n-coil links) between the transmitter (Tx) and the receiver (Rx), has been extensively studied [5]–[7], demonstrating that it is an effective method

This work was supported in part by CAP and CSIC from Universidad de la República, Uruguay, and by the French National Research Agency ANR-21-CE19-0015-01.

Andrés Seré and Leonardo Steinfeld are with the Instituto de Ingeniería Eléctrica, Facultad de Ingeniería, Universidad de la República, Montevideo, Uruguay (e-mail: asere@fing.edu.uy; leo@fing.edu.uy).

Simon Hemour is with the IMS Laboratory, University of Bordeaux, Bordeaux, France (e-mail: simon.hemour@u-bordeaux.fr).

Pablo Pérez-Nicoli is with the Instituto de Ingeniería Eléctrica, Facultad de Ingeniería, Universidad de la República, Montevideo, Uruguay, and also with the IMS Laboratory, University of Bordeaux, Bordeaux, France (e-mail: pablop@fing.edu.uy).

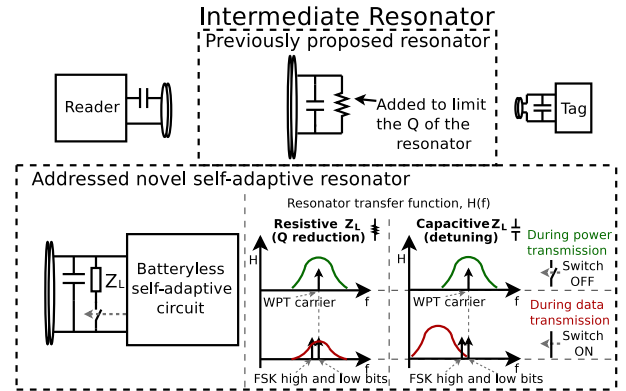


Fig. 1. Block diagram of the proposed self-adaptive resonator.

to improve link efficiency and transmission distance. From an intuitive perspective, we may consider the intermediate resonator to operate analogously to a repeater/relay. Due to its resonant nature, it is easily excited at the carrier frequency, and the resulting induced current also contributes to generating magnetic field. Furthermore, it has been demonstrated that these resonators are not only beneficial when positioned in intermediate locations; many studies incorporate resonators in the same plane as the Tx or Rx coil [1], [8], [9] to enhance various performance characteristics of the link.

The larger the quality factor (Q) of the intermediate resonator(s), the Tx, and Rx coils, the higher the efficiency that can be achieved by the link. On the other hand, a high-Q reduces the bandwidth of the link, affecting data transmission over it. The higher the Q of a resonator, the longer it takes for an oscillation to decay after the excitation source is turned off. This causes each bit transmitted in the link to take longer to decay and remain oscillating in high-Q resonators, thereby interfering with the next transmitted bit. This is an undesired phenomenon known as inter-symbol interference (ISI).

One approach to mitigate ISI is to transmit suppression pulses after each bit, aiming to decrease the amplitude of the transmitted bit before sending the next one [10]–[12]. This solution complicates the data transmitter implementation and requires the use of extra energy to actively dampen the sent pulses. This may not be viable in some applications, such as RFID, where the energy availability at the tag is low. Additionally, in many applications, there are already numerous tags in use, and replacing them may be impractical. Therefore, it is preferable to propose changes to the reader

or the intermediate resonator. A simpler solution, which is currently used in low-frequency RFID systems, is to limit the Q of the coils used to values that enable communication, albeit at the expense of reducing the power transfer efficiency [4].

In this paper, we present a novel resonator that can maintain a tuned high- Q response while energy is being transferred and automatically attenuates its response when data transmission starts. The proposed resonator is utilized in a low-frequency RFID system that is widely employed for cattle identification, forming a 3-coil link. Fig. 1 depicts a diagram of the RFID system used. When an intermediate resonator is not used, the system, which is an actual commercial RFID low-frequency system, achieves a reading distance of 16 cm. In [4], a resonator with limited Q was designed to enhance efficiency without affecting data transmission, thereby increasing the reading distance to 43 cm. In this study, we employed the same reader, intermediate resonator, and tag used in [4]. However, rather than introducing a resistor that constantly decreases the Q of the intermediate resonator, we implemented the proposed self-adaptive circuit that only reduces Q (by adding a resistor) when necessary (during data transmission). Moreover, we also evaluate the performance of adding a capacitive element, instead of a resistor, thereby detuning the intermediate resonator instead of reducing its Q , which was proved to achieve a larger reading distance. The impact on the ISI of introducing a resistive or capacitive element into the resonator is further elucidated in Section III-C. Compared to using the regular limited Q intermediate resonator proposed in [4], the proposed self-adaptive resonator increases the maximum reading distance by $\approx 50\%$ (from 43 cm to 65 cm).

The concept behind implementing this 3-coil cattle RFID system is to position the intermediate resonator at one or more locations along the cattle chute or cattle loading ramp. This simplifies or even enables the automation of the reading process using a handheld reader. It is worth emphasizing that while this article implements the self-adaptive resonator for a specific RFID link, the proposed concept of using intermediate resonators capable of dynamically adjusting their Q or resonance frequency can be applied to other systems.

Dynamic Tx or Rx adjustments have been extensively employed for various purposes, including resonance tuning [13]–[15], output voltage regulation [16], and enhancing power or link efficiency [17], [18]. However, there are only a few instances in the literature where an intermediate resonator is dynamically adapted [8], [9]. Furthermore, these previous works involve a wired connection between Rx and the intermediate coil, which is not the case in this study. Additionally, the modification of the intermediate resonator is carried out for a different purpose; [8] tries to deal with a varied distance range, alignment, and load impedance in real-time, while [9] aims to implement constant current and constant voltage sources for charging a battery.

This paper is organized as follows. First, in Section II, the RFID system used as a proof-of-concept is presented. Next, in Section III, we delve into the design of the self-adaptive intermediate resonator. Measurements of the RFID system and the most critical signals involved are outlined in Section IV. Finally, Section V summarizes the main conclusions.

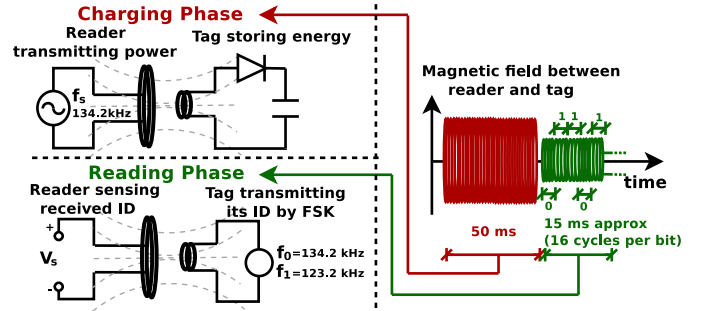


Fig. 2. Graphic illustration of the operating principle of the half-duplex RFID system used in this work.

II. LOW-FREQUENCY RFID LINK DESCRIPTION

In these cattle RFID systems, the charging phase (energy transmission from the reader to the tag) and the reading phase (data transmission from the tag to the reader) are time-interleaved, which is known as half-duplex communication. Fig. 2 graphically illustrates the operation of the link, which is described below. The charging phase operates at a carrier frequency of 134.2 kHz and typically spans 50 ms. After this elapsed time, the reader halts coil excitation, swapping the voltage driver for a sensing circuit to detect the tag's response. The tag rectifies the received signal during the charging phase, storing the energy in a capacitor. The tag identifies the end of the charging phase by detecting the absence of induced voltage in its antenna. Subsequently, the tag utilizes the stored energy in the capacitor to respond with its unique identification number (reading phase), employing FSK modulation (134.2 kHz and 123.2 kHz for the 0 and 1 bits, respectively). During the reading phase, the tag transmits each bit for 16 cycles, and the transmission of the entire ID takes approximately 15 ms [4], [6].

In these half-duplex communication systems, the reading process can fail due to two reasons: 1) the tag does not receive enough energy to transmit its complete ID, which will be referred to as “Charging limit”, or 2) the reader is unable to receive and decode the tag's transmitted ID correctly, which will be referred to as “Reading/decoding limit”. In the 2-coil RFID link described here, the reading range is limited by the charging phase. Beyond approximately 16 cm, the energy received by the tag is insufficient, thus, the transmission of its ID is interrupted (due to the insufficient energy) before completion.

This 2-coil RFID link system avoids ISI due to having the Q of the coils limited by design. However, when an intermediate resonator is included, there is a risk of introducing ISI if its Q value is not carefully controlled. In [4], a maximum reading distance of 43 cm was achieved by designing a Q -limited resonator. For distances larger than 43 cm, a higher Q is required to energize the tag, resulting in ISI that impedes the reader's to decode the received signal. Lowering the Q to mitigate ISI prevents the tag from achieving full energization. This trade-off in Q , which results in the two different non-reading situations (“Reading/decoding” and “charging” limits), is visually depicted in Fig. 3.

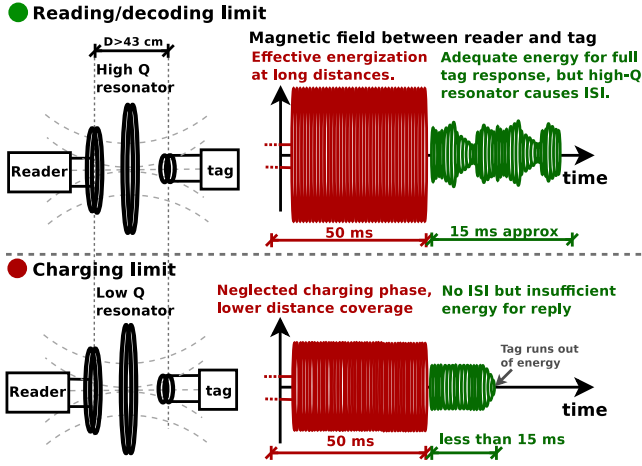


Fig. 3. Illustration of the trade-off in selecting the quality factor (Q) of the intermediate coil: a high-Q generates ISI, whereas a low-Q prevents the tag from fully charging.

III. PROPOSED SELF-ADAPTIVE CIRCUIT

A. Main idea

This paper presents the design and implementation of a novel batteryless resonator capable of self-adjusting its response (either its Q or resonant frequency) to surpass the trade-off discussed in the preceding section and depicted in Fig. 3.

The magnetic field produced by the reader during the charging phase is significantly greater than that generated by the tag during the reading phase. Consequently, the intermediate resonator detects the end of the charging phase by recognizing the falling edge of the magnetic field envelope, as depicted in Fig. 4. At this point, and for a duration longer than the tag's response time (15 ms), to prevent the occurrence of ISI, an impedance Z_L is introduced in parallel to the intermediate coil, whether resistive or capacitive, as further discussed in Section III-C.

B. Proposed circuit

The system described in Fig. 4 is implemented by the circuit shown in Fig. 5, where L_A and R_A model the intermediate resonator coil with its equivalent series resistance, and C_A is a capacitor adjusted to achieve resonance at the power carrier frequency (134.2 kHz). MOSFETs M_1 and M_2 work as switches; when they turned on, the impedance Z_L is added in parallel with the L_A - C_A resonator. The diodes D_1 to D_4 form a full-wave rectifier. Resistor R_1 limits the energy taken from the inductive link, and, in conjunction with R_2 , C_1 and the diodes, implements an envelope detector, V_{C1} . Capacitor C_S stores the peak of the envelope and, also, the necessary energy to power-on the transistors M_1 and M_2 . When the envelope (V_{C1}) falls, it turns on the thyristor implemented through Q_1 and Q_2 , resulting in the activation of transistors M_1 and M_2 . Resistors R_3 and R_4 are pull-downs and the zener diode D_Z limits the voltage to avoid damaging the transistors. The full-wave rectifier ensures that the source of the MOSFET transistors (and hence its body) are at the minimum circuit potential (neglecting the diodes voltage dropout).

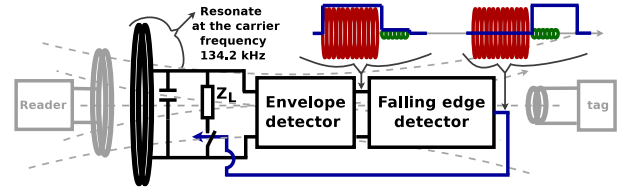


Fig. 4. Graphical representation of the proposed self-adaptive resonator.

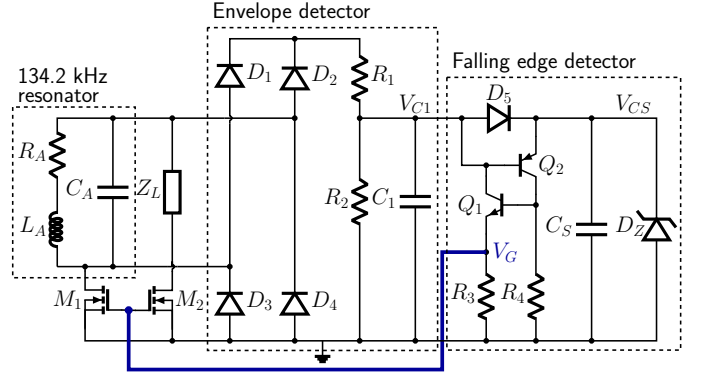


Fig. 5. Schematic of the self-adaptive resonator circuit (operation is illustrated in Fig. 4). $L_A \approx 648 \mu\text{H}$, $R_A \approx 13.3 \Omega$, $C_A \approx 2.17 \text{ nF}$, M_1 and M_2 are ZVNL120A, $D_{1..5}$ are 1N4148, $R_1 = 100 \text{ k}\Omega$, $R_{2..4} = 1 \text{ M}\Omega$, $C_1 = 1 \text{ nF}$, Q_1 is BC547, Q_2 is BC557, $C_S = 100 \text{ nF}$ and $V_Z = 16 \text{ V}$.

C. Impedance Z_L discussion

In this section, it is discussed why detuning the intermediate resonator (capacitive Z_L) also proves effective in addressing ISI, similar to reducing the quality factor (resistive Z_L).

To grasp this discussion, it is important to recall that during the reading phase, the bit 0 is encoded at the same frequency as the power carrier used during the charging phase (134.2 kHz), thus aligning with the resonant frequency of the intermediate coil. In contrast, bit 1 is encoded at a lower frequency (123.2 kHz). Therefore, if the intermediate resonator keeps the same resonant frequency (134.2 kHz) during charging and reading phase, the bit 0 (134.2 kHz) will pass through a high-Q resonator, reaching larger amplitudes than the bit 1 (123.2 kHz), which will confront a non-resonant intermediate coil. This difference in amplitudes, combined with having a long decay time (due to a high Q), sets up a scenario favorable to ISI, as when a bit 1 is sent after a bit 0, the non-resonant 1 will be overshadowed by the preceding resonant 0.

If we use a resistive Z_L , the Q of the resonator for both bits 0 and 1 will decrease. Therefore, while we will succeed in reducing the decay time and avoiding ISI, we will further impair the transmission conditions for bit 1. Consequently, the RMS voltage received from bit 1, V_S in Fig. 2, will be very low, potentially preventing the reader from decoding the signal. A similar effect will occur if we add a capacitive Z_L that significantly alters the resonator frequency, as it would yield a comparable effect to removing the resonator. However, if we use a capacitive Z_L that shifts the resonator frequency to a value near the middle of the 0 and 1 bits, the amplitude imbalance between the bits is addressed, preventing one bit from overshadowing the other.

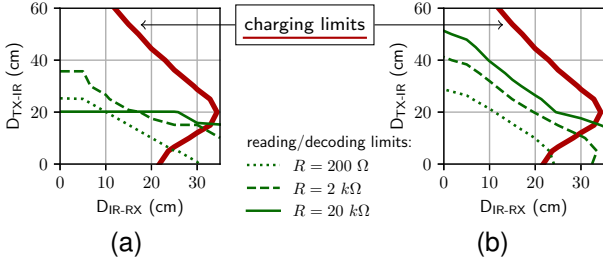


Fig. 6. Simulation results for the reading/decoding limits using different resistances as Z_L (Fig. 5). The charging limit indicates not enough power received during the charging phase. (a) Reading/decoding limits due to ISI. (b) Reading/decoding limits due to a too low sensed voltage (V_S in Fig. 2).

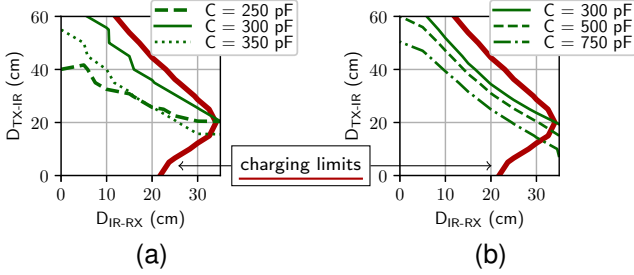


Fig. 7. Simulation results for the reading/decoding limits using different capacitances as Z_L (Fig. 5). The charging limit indicates not enough power received during the charging phase. (a) Reading/decoding limits due to ISI. (b) Reading/decoding limits due to a too low sensed voltage (V_S in Fig. 2).

Figs. 6 (resistive Z_L) and 7 (capacitive Z_L) substantiate the previous discussion through LTspice simulations, employing the models for Tx and Rx introduced in [4], along with the proposed resonator (Fig. 5). These plots depict the maximum distances D_{TX-IR} (reader-to-intermediate resonator) and D_{IR-RX} (intermediate resonator-to-tag) beyond which the tag cannot be read. Figs. 6a and 7a indicate the limit from which the bit error rate (BER) is not null due to the presence of ISI, while Figs. 6b and 7b indicate the limit due to a low received signal amplitude. As explained earlier, reading may also fail if the tag is not fully energized during the charging phase, thus, this charging limit was also superimposed in all the figures.

To analyze the curves plotted in Figs. 6 and 7, it is important to note that the higher up to the right they are positioned, the greater the distances between the coils can be to read the tag. Conversely, the lower to the left they are, the shorter the achievable read distance. Firstly, it is noteworthy that merely reducing the bit decay time by introducing a resistive element (Fig. 6) still results in strong limitations on reading distances due to ISI (Fig. 6a). This is because the amplitude of the resonant bit (0) remains significantly higher than that of the non-resonant bit (1), overshadowing it. Moreover, as the decay time is decreased (lower R in parallel, thus lower Q), the reduction on the received bit amplitudes becomes more pronounced, which also restricts the reading distance (Fig. 6b). However, by modifying the resonance frequency, as illustrated in Fig. 7, curves positioned higher to the top right are achieved, corresponding to greater reading distances. As seen in Fig. 7, the optimal value for C is 300 pF, which corresponds to setting the intermediate coil resonance frequency near the middle of the 0 and 1 bits. Both higher and lower values of C result in more restrictive distance limits, as also shown in Fig. 7.

Therefore, as a result of the analysis, a standard 330 pF capacitor was used as Z_L , thus completing the design of the proposed circuit presented in Fig. 5.

IV. MEASUREMENT RESULTS

The self-adaptive resonator, addressed in the previous section (Fig. 5, with a capacitive Z_L of 330 pF as designed), was used to increase the reading distance of the low frequency RFID link described in Section II. The measurement setup is shown in Fig. 8, corresponding to one of the various coil arrangements acquired. Fig. 9 plots the simulated limits introduced in the previous section (continuous line) overlapped with the measurement results (solid dots), showing good agreement and validating the analysis. The cause of the reading failure (“Charging limit” or “reading/decoding” limit) discussed in Section II was determined through measurements, as represented by the colors indicated in the legend, which is also consistent with the simulations.

To further validate the proposed circuit, it was measured during operation while also sensing the magnetic field by a sniffer antenna connected to an oscilloscope. These measurement results are presented in Figs. 10 and 11 and described in the remainder of this section. Fig. 10 shows the magnetic field, the voltage V_{CS} (at C_S terminals) and the MOSFETs gate voltage (V_G). It shows the capacitor C_L charging-up during the 50 ms of the charging phase and, at the end of this phase, when the envelope of the magnetic field has a falling edge, the thyristor formed by Q_1 and Q_2 turns on the MOSFETs M_1 and M_2 (gate voltage V_G rises). The difference between V_{CS} and V_G during the reading phase corresponds to the thyristor (Q_1 & Q_2) voltage drop. Fig. 11 compares the case in which the intermediate resonator is connected only to a capacitor forming a *high-Q LC resonator* at 134.2 kHz (light gray shadow); the case in which the intermediate resonator is connected not only

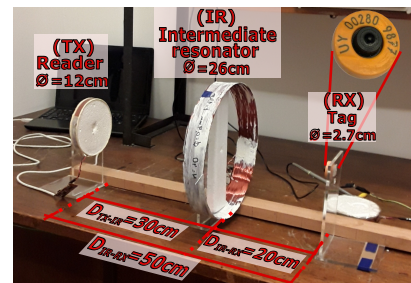


Fig. 8. Measurement setup. The maximum read distance corresponds to $D_{TX-IR} = 60$ cm and $D_{IR-RX} = 5$ cm.

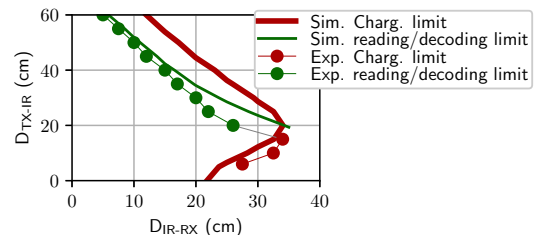


Fig. 9. Measurement results.

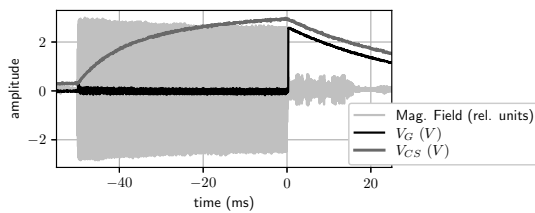


Fig. 10. Circuit measurement using an auxiliary coil as magnetic field sniffer. Nodes V_G and V_{CS} are labeled in Fig. 5.

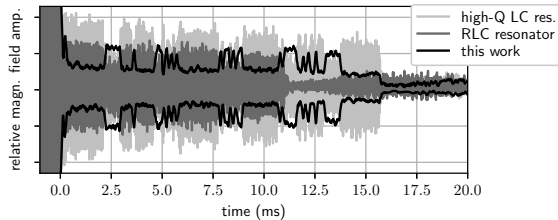


Fig. 11. Tag response for different intermediate coil: high-Q LC resonator, RLC limited-Q resonator [4], and the detuned resonator used in this work.

to a capacitor to achieve resonance at 134.2 kHz, but also to a parallel resistance of 53 k Ω to reduce its Q, forming the *RLC resonator* proposed in [4] (strong gray shadow); and the case in which the proposed self-adaptive circuit is used (only the black envelope is shown for clarity purpose). With the first setup (*high-Q LC resonator*) the tag is correctly energized (its answer takes around 15 ms) but there is a strong ISI (not showed in the image but the reader don't returns lectures). The second setup (*RLC resonator*) shows an answer which takes significantly less than 15 ms proving that the tag was not energized enough to complete its ID transmission. Finally, the proposed self-adaptive resonator, has a 15 ms answer time, without ISI (reader returns lectures), and also shows that the resonance frequency during the reading phase is more near the 123.2 kHz than the 134.2 kHz, contrary to the others two cases (the amplitude ratios are opposite). This is consistent with the aim of the proposed design that reduce the resonance frequency to avoid the ISI during the reading phase.

V. CONCLUSION

This work contributes by proposing a novel resonator that can dynamically adjust its response (either its Q or resonant frequency) to enhance both power and data transmission over the same inductive link. It is composed of a simple batteryless circuit that harnesses the power generated by the inductive link. This circuit can maintain a high-Q resonator for efficient power transmission and self-adapt to enable proper data transmission. Furthermore, we demonstrated that, due to the FSK modulation, adjusting the resonance frequency, rather than introducing dissipative elements like resistors to decrease the Q, is a more effective strategy. The validity of the proposed concept was confirmed through measurements conducted on an actual RFID system extensively employed for cattle identification, leading to a substantial improvement in the reading distance (50% greater reading range compared to using a classic fixed-Q intermediate resonator).

REFERENCES

- [1] Q. Wang, W. Che, M. Mongiardo, and G. Monti, "Wireless power transfer system with high misalignment tolerance for bio-medical implants," *IEEE Transactions on Circuits and Systems II: Express Briefs*, vol. 67, no. 12, pp. 3023–3027, 2020.
- [2] S. Pal and W.-H. Ki, "40.68 MHz digital on-off delay-compensated active rectifier for WPT of biomedical applications," *IEEE Transactions on Circuits and Systems II: Express Briefs*, vol. 67, no. 12, pp. 3307–3311, 2020.
- [3] A. Celentano, C. Paolino, F. Pareschi, L. Callegaro, R. Rovatti, and G. Setti, "Mutual inductance measurement in wireless power transfer systems operating in the MHz range," *IEEE Transactions on Circuits and Systems II: Express Briefs*, pp. 1–1, 2023.
- [4] P. Pérez-Nicoli, A. Rodríguez-Esteva, and F. Silveira, "Bidirectional analysis and design of RFID using an additional resonant coil to enhance read range," *IEEE Transactions on Microwave Theory and Techniques*, vol. 64, no. 7, pp. 2357–2367, 2016.
- [5] M. Kiani and M. Ghovanloo, "The circuit theory behind coupled-mode magnetic resonance-based wireless power transmission," *IEEE Transactions on Circuits and Systems I: Regular Papers*, vol. 59, no. 9, pp. 2065–2074, 2012.
- [6] P. Pérez-Nicoli, F. Silveira, and M. Ghovanloo, *Inductive Links for Wireless Power Transfer: Fundamental Concepts for Designing High-efficiency Wireless Power Transfer Links*. Cham: Springer International Publishing, 2021. [Online]. Available: <https://link.springer.com/10.1007/978-3-030-65477-1>
- [7] C.-J. Chen, T.-H. Chu, C.-L. Lin, and Z.-C. Jou, "A study of loosely coupled coils for wireless power transfer," *IEEE Transactions on Circuits and Systems II: Express Briefs*, vol. 57, no. 7, pp. 536–540, 2010.
- [8] Y. Zhao, H. Li, S. Naderiparizi, A. Parks, and J. R. Smith, "Low-cost wireless power efficiency optimization of the NFC tag through switchable receiver antenna," *Wireless Power Transfer*, vol. 5, no. 2, pp. 87–96, 2018.
- [9] Y. Li, J. Hu, M. Liu, Y. Chen, K. W. Chan, Z. He, and R. Mai, "Reconfigurable intermediate resonant circuit based wpt system with load-independent constant output current and voltage for charging battery," *IEEE Transactions on Power Electronics*, vol. 34, no. 3, pp. 1988–1992, 2018.
- [10] M. Schormans, D. Jiang, V. Valente, and A. Demosthenous, "Short-range quality-factor modulation (squirm) for low power high speed inductive data transfer," *IEEE Transactions on Circuits and Systems I: Regular Papers*, vol. 66, no. 9, pp. 3254–3265, 2019.
- [11] M. Kiani and M. Ghovanloo, "A 20-Mb/s pulse harmonic modulation transceiver for wideband near-field data transmission," *IEEE Transactions on Circuits and Systems II: Express Briefs*, vol. 60, no. 7, pp. 382–386, 2013.
- [12] F. Inanlou, M. Kiani, and M. Ghovanloo, "A 10.2 Mbps pulse harmonic modulation based transceiver for implantable medical devices," *IEEE journal of solid-state circuits*, vol. 46, no. 6, pp. 1296–1306, 2011.
- [13] B. Lee, M. Kiani, and M. Ghovanloo, "A triple-loop inductive power transmission system for biomedical applications," *IEEE transactions on biomedical circuits and systems*, vol. 10, no. 1, pp. 138–148, 2015.
- [14] W. Redman-White, H. Kennedy, R. Bodnar, and T. Lee, "Adaptive tuning of large-signal resonant circuits using phase-switched fractional capacitance," *IEEE Transactions on Circuits and Systems II: Express Briefs*, vol. 64, no. 9, pp. 1072–1076, 2017.
- [15] F. Kong, M. Ghovanloo, and G. D. Durgin, "An adaptive impedance matching transmitter for a wireless intraoral tongue-controlled assistive technology," *IEEE Transactions on Circuits and Systems II: Express Briefs*, vol. 67, no. 2, pp. 240–244, 2020.
- [16] J. Tian and A. Hu, "Stabilising the output voltage of wireless power pickup through parallel tuned dc-voltage controlled variable capacitor," *Electronics Letters*, vol. 52, no. 9, pp. 758–759, 2016.
- [17] P. P. Mercier and A. P. Chandrakasan, "Rapid wireless capacitor charging using a multi-tapped inductively-coupled secondary coil," *IEEE Transactions on Circuits and Systems I: Regular Papers*, vol. 60, no. 9, pp. 2263–2272, 2013.
- [18] Z. Dang, Y. Cao, and J. A. A. Qahouq, "Reconfigurable magnetic resonance-coupled wireless power transfer system," *IEEE Transactions on Power Electronics*, vol. 30, no. 11, pp. 6057–6069, 2015.